Modern Mechanical Engineering, 2011, 1, 84-92
doi:10.4236/mme.2011.12011 Published Online November 2011 (http://www.SciRP.org/journal/mme)

Design, Development and Testing of an Air Damper to Control the Resonant Response of a SDOF Quarter-Car Suspension System

Ranjit G. Todkar
Department of Mechanical Engineering, *P.V.P. Institute of Technology*, *Sangli*, *India*
E-mail: *rgtodkar@gmail.com*
Received October 21, 2011; *revised November* 3, 2011; *accepted November* 10, 2011

Abstract

An air damper possesses the advantages that there are no long term changes in the damping properties, there is no dependence on working temperature and additionally, it has less manufacturing and maintenance costs. As such, an air damper has been designed and developed based on the Maxwell type model concept in the approach of Nishihara and Asami and Nishihara [1]. The cylinder-piston and air-tank type damper characteristics such as air damping ratio and air spring rate have been studied by changing the length and diameter of the capillary pipe between the air cylinder and the air tank, operating air pressure and the air tank volume. A SDOF quarter-car vehicle suspension system using the developed air enclosed cylinder-piston and air-tank type damper has been analyzed for its motion transmissibility characteristics. Optimal values of the air damping ratio at various values of air spring rate have been determined for minimum motion transmissibility of the sprung mass. An experimental setup has been developed for SDOF quarter-car suspension system model using the developed air enclosed cylinder-piston and air-tank type damper to determine the motion transmissibility characteristics of the sprung mass. An attendant air pressure control system has been designed to vary air damping in the developed air damper. The results of the theoretical analysis have been compared with the experimental analysis.

Keywords: Ride Comfort, Quarter-Car Suspension Model, Cylinder-Piston and Air-Tank Type Air Damper, Motion Transmissibility, Optimal Air Damping Ratio

1. Introduction

The control of response of the sprung mass of a SDOF quarter-car suspension system subjected to the road excitation is necessary in the neighborhood of the resonance for the better ride comfort, road holding and stability. Various damping mechanisms such as, hydraulic, electromagnetic, ER and MR fluid and air dampers have been reported in the literature [1-3]. In this paper, an air enclosed cylinder-piston and air-tank type air damper configuration has been selected for design and development because in these dampers there are no long term changes in the damping properties, no dependence on working temperature. Air dampers have less manufacturing and maintenance costs. A SDOF quarter-car vehicle suspension model using such a developed air damper has been analyzed for its motion transmissibility characteristics. The air damper has been designed and developed as a Maxwell type model in the approach of Nishihara and Asami and Nishihara [1]. The air damper characteristics such as air damping ratio and air spring rate have been studied. Optimal values of the air damping ratio at various values of air spring rate have been determined to obtain minimum motion transmissibility of the sprung mass. An experimental setup for SDOF quarter-car suspension system using the developed air enclosed cylinder-piston and air-tank type damper has been developed with an attendant air pressure control system.

2. Development of an Air Enclosed Cylinder-Piston and Air-Tank Type Damper

A cylinder-piston and air-tank type damper, both the sides of which are connected to two surge tanks through capillary pipes has been developed. The arrangement is used to set the desired damping properties by allowing the changes in 1) Tank volume to cylinder volume ratio Nt, 2) Operating air pressure pi, and 3) Capillary pipe length l_{pipe} and diameter d_{pipe}. **Figure 1(a)** shows a cylinder-piston and air-tank type air damper. **Figure 1(b)** shows the mathematical models for the air Damper [4].

2.1. Air Spring Rate k_a [3]

$$k_a = \frac{2\,n\,pi\,s^2}{v_t} = \left[\frac{2\,n\,s^2}{v_c}\right]\left[\frac{pi}{Nt}\right]$$

where $v_t = v_c Nt$ (1)

where n is the index of expansion of air, pi is the operating air pressure in the system, s is the cross sectional area of the piston, v_t is the air tank volume and v_c is the air cylinder volume.

Let air spring rate ratio $k = \left[\frac{k_a}{k_1}\right]$ (2)

where k_1 is the suspension spring rate.

Substituting the value of k_a from Equation (1) in Equation (2), we obtain $k = \left[\frac{2\,n\,s^2}{v_c k_1}\right]\left[\frac{pi}{Nt}\right]$ where

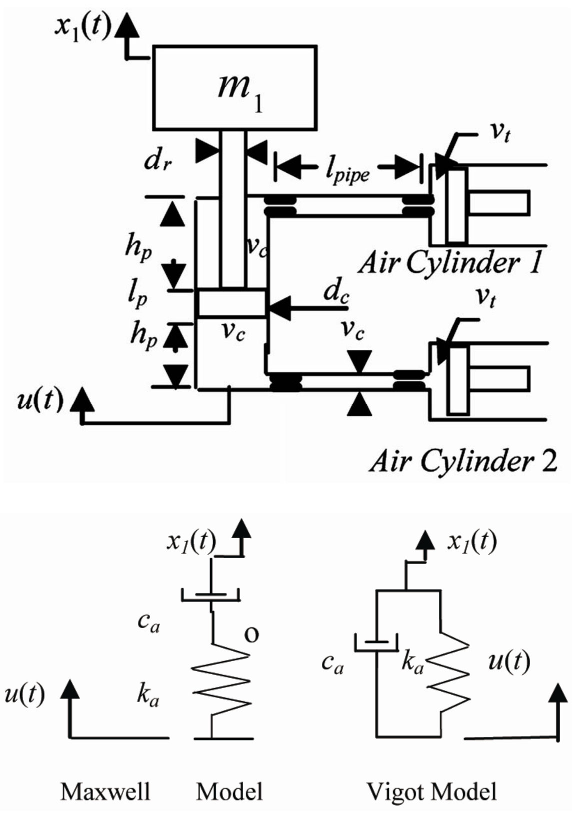

Figure 1. (a) Cylinder-piston and air tank type system; (b) Mathematical models.

$$s = \frac{\pi}{4}\left(d_p^2 - d_r^2\right) \text{ and } v_c = s\,h_p \quad (3)$$

where d_p is the piston diameter and d_r is the piston rod diameter and h_p is the height of the cylinder volume.

Defining the terms p_1, p_2 and p_3 as

$p_1 = \frac{d_p}{d_c}$, $p_2 = \frac{d_r}{d_c}$ and $p_3 = \frac{h_p}{d_c}$ and substituting the values of p_1, p_2, p_3, s and v_c in Equation (3), we obtain

$$k = \frac{n\,\pi}{2\,p_3\,k_1}\left[p_1^2 - p_2^2\right]\left[d_c\right]\left[\frac{pi}{Nt}\right] \quad (4)$$

Assuming the values $p_1 = 0.985$, $p_2 = 0.333$, $p_3 = 0.5$ and $k_1 = 970$ N/m, the Equation (4) becomes.

$$k = 0.00403146\left[d_c\right]\left[\frac{pi}{Nt}\right] \quad (5)$$

2.1.2. Air Damping Ratio ζ_a [3]

$$\zeta_a = \left[\frac{w_a v_t}{2\,n\,c_r\,pi}\right] \text{ where } w_a = \left[\frac{k_a}{m_1}\right]^{1/2} \quad (6)$$

The capillary flow coefficient c_r is given as

$$c_r = \left[\frac{\pi\left(d_{pipe}\right)^4}{128\,\mu_o\,l_{pipe}}\right] \text{ (Refer [3])} \quad (7)$$

in which d_{pipe} and l_{pipe} are the capillary pipe diameter and length respectively and μ_o is the viscosity of air at atmospheric temperature. Taking the value of k_a from Equation (1) and substituting it in Equation (6), we get

$$w_a = \left[\frac{2\,n\,pi\,s^2}{v_c\,Nt\,m_1}\right]^{1/2} = s\sqrt{\left[\frac{2\,n}{v_c\,m_1}\right]}\sqrt{\left[\frac{pi}{Nt}\right]} \quad (8)$$

Substituting w_a from Equation (8) and c_r from Equation (7) in Equation (6)

we obtain

$$\zeta_a = \left[\frac{\left[s\sqrt{\frac{2\,n}{v_c\,m_1}}\sqrt{\frac{pi}{Nt}}\right]\left[v_c\,Nt\right]}{2\,n\left[\frac{\pi\left(d_{pipe}\right)^4}{128\,\mu_o\,l_{pipe}}\right]pi}\right] \text{ or}$$

$$\zeta_a = Q_1\left[\frac{l_{pipe}}{\left(d_{pipe}\right)^4}\right]\frac{1}{\sqrt{\frac{pi}{Nt}}} \quad (9)$$

where $Q_1 = \left[\frac{128\,\mu_o\,s}{\pi}\right]\left[\sqrt{\frac{v_c}{2\,n\,m_1}}\right]$

Similarly using expressions (4) and (9) respectively for k and ζ_a one can write

$$\zeta_a = Q_2 \frac{1}{\sqrt{k}} \tag{10}$$

where $$Q_2 = \frac{w_1\left[\frac{1}{4}\left(d_p^2 - d_r^2\right)\right]^2 \left(128\,\mu\, l_{pipe}\right)}{\left(d_{pipe}\right)^4}$$

2.2. Air Damper Characteristics

From Equation (10), it is seen that ζ_a will be large for small values of k, *i.e.* for small values of k_a for given value of k. To provide variable damping ratio, the value of k can be varied. For the application of this device as a variable damping unit smaller values of k (0.05 to 0.125) are preferred. Also k depends on the ratio *(pi/Nt),* (refer Equation (4)) *i.e.* for small values of k, ratio *(pi/Nt)* should be kept small.

2.2.1. Effect of the Cylinder Diameter d_c on Air Spring Rate Ratio k (Refer Figure 2)

Here d_c is varied as d_c = 10 mm, d_c = 20.0 mm and d_c = 30.0 mm. The values of d_r = (0.333) (d_c) = (0.333) (30.0) = 10mm and h_p =(0.5) (d_c)= (0.5) (30.0) = 15 mm have been obtained. Considering a sliding fit between the piston and cylinder the piston diameter d_p is taken as 29.95 mm for a cylinder diameter d_c = 30 mm. **Figure 2** shows the effect of variation of cylinder bore d_c on spring rate ratio k .

2.2.2. Effect of d_{pipe} on ζ_a (Refer Figure 3)

Using the Equation (10), the effect of variation of ratio on air damping ratio ζ_a has been obtained for the values of d_{pipe} = 2.5, 2.0 and 1.5 mm. with l_{pipe} = 3.0 m. **Figure 4** shows the effect of air spring rate ratio k on the air damping ratio ζ_a. for the values of d_{pipe} = 2.5, 2.0 and 1.5 mm. with l_{pipe} = 3.0 m .

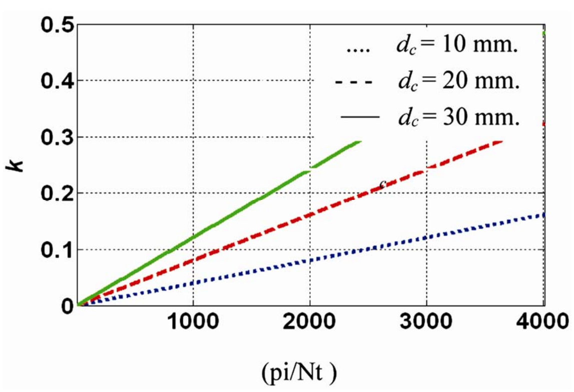

Figure 2. ***k*** **vs (*pi/Nt*) for different values of d_c = a) 10 mm, b) 20 mm, c) 30 mm**.

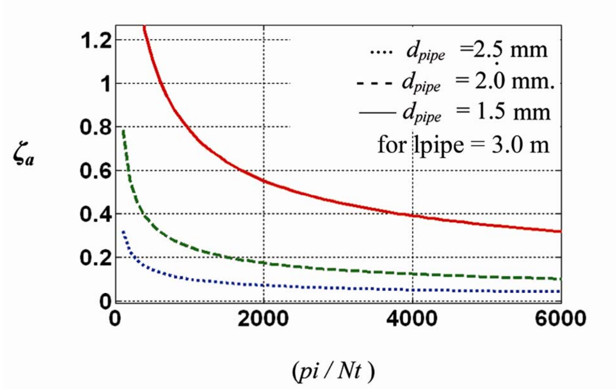

Figure 3. ζ_a ***vs*** **(*pi/Nt*) with l_{pipe} = 3.0 m d_{pipe} = a) 2.5 mm, b) 2.0 mm, c) 1.5mm.**

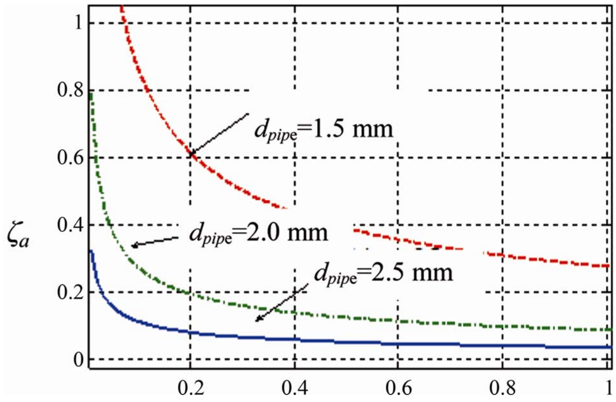

Figure 4. ζ_a ***vs k*** **with l_{pipe}=3.0 m and d_{pip} = a) 2.5 mm, b) 2.0 mm, c) 1.5mm.**

From the curves of **Figures 2**, **3** and **4**, it is seen that the developed air damper can provide appreciable increase in the damping ratio for values of the ratio (*pi/Nt*) in the range 500 to 6000 N/sq.m. per unit volume ratio (v_t/v_c).

2.2.3. Developed Air Damper Specifications

Plate 1 shows the details of the air damper cylinder and slider assembly and air damper piston rod fitted to the sprung mass assembly .The air damper has been developed with the physical dimensions given in **Table 1**.

A double acting air cylinder configuration has been selected with the piston travel of ±15 mm amplitude. The base excitation of ±1.5mm amplitude is provided. The material used for the entire assembly is steel with EN8 series, properly ground and finished to the selected dimensions. The sprung mass is in the form of a circular plate made up of C.I.

2.2.4. SDOF Quarter Car Vehicle Suspension System Model [5]

Thus the developed cylinder-piston and air tank-type air damper is capable of providing variable damping ratio.

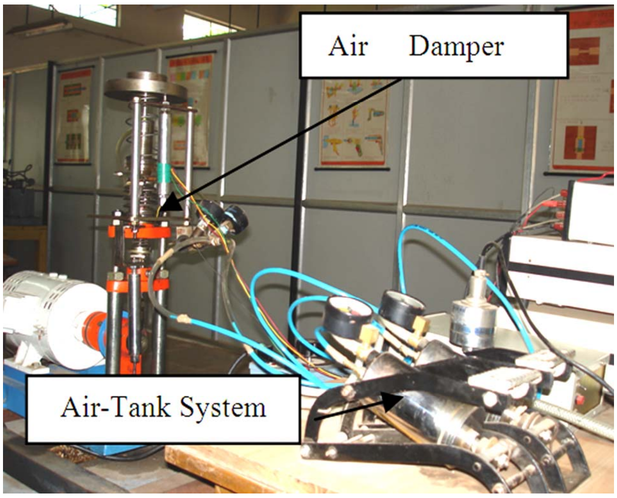

Plate 1. Air damper cylinder-piston and air-tank system.

Table 1. Air damper dimensions.

d_c	d_p	d_r	h_p	l_p
30	29.85	10	15	13

Figures 5(a) and **(b)** show a SDOF quarter-car vehicle suspension system model with system damping only and using the developed air damper respectively described in Section 2, respectively.

2.3. Equations of Motion

The equations of motion are given below

1) For **Case 1** the equation of motion is

$$m_1\ddot{x}_1 = -k_1(x_1 - u) - c_1(\dot{x}_1 - \dot{u}) \tag{11}$$

2) For **Case 2** the equations of motion are

$$m_1\ddot{x}_1 = -k_1(x_1 - u) - c_1(\dot{x}_1 - \dot{u}) - c_a(\dot{x}_1 - \dot{y}) \tag{12}$$

$$-c_a(\dot{y} - \dot{x}_1) - k_a(\dot{y} - \dot{u}) = 0 \tag{13}$$

2.4. Motion Transmissibility of the Sprung Mass

Assume the steady state solutions of the Equations (11), (12) and (13) in the form $x_1 = X_1e^{jwt}$, $x_2 = X_2e^{jwt}$ and the base excitation as $u = Ue^{jwt}$, and following the usual procedure of solution, the expression for the motion transmissibility Mt1 (for the sprung mass) has been obtained for Case 1 as

$$\mathrm{Mt1} = \frac{X_1}{U} = \sqrt{\left[\frac{[A_0]^2 + [A_1\lambda]^2}{\left[B_0 - B_2\lambda^2\right]^2 + [B_1\lambda]^2}\right]} \tag{14}$$

where $A_1 = 2\zeta_1$, $A_0 = 1$, $B_2 = 1$, $B_1 = 2\zeta_1$ and $B_0 = 1$ and for Case 2 as

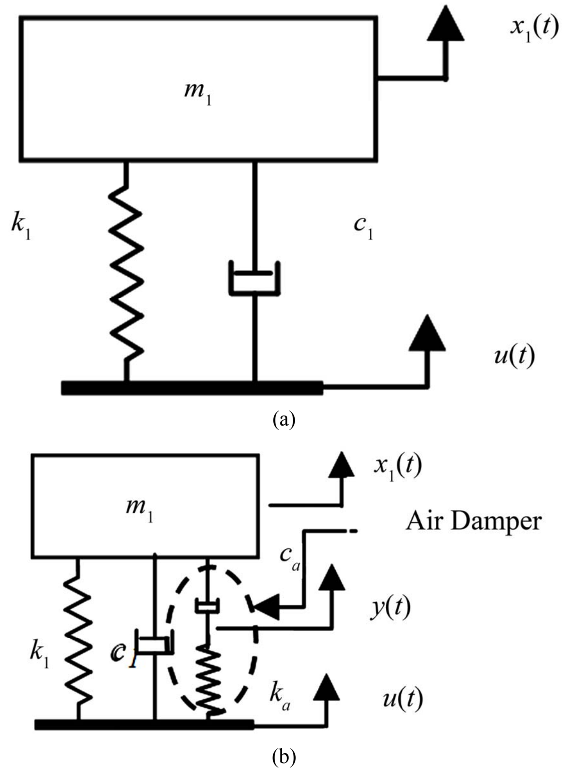

Figure 5. SDOF quarter-car vehicle suspension system model. (a) SDOF quarter-car vehicle suspension System with system damping; (b) SDOF quarter-car vehicle suspension system with system damping and air damper with maxwell type model.

$$\mathrm{Mt1} = \frac{X_1}{U} = \sqrt{\left[\frac{\left[-a_2\lambda^2 + a_0\right]^2 + [a_1\lambda]^2}{\left[b_0 - b_2\lambda^2\right]^2 + \left[-b_3\lambda^3 + b_1\lambda\right]^2}\right]} \tag{15}$$

where $a_2 = 2(\zeta_1 + \sqrt{k}\,\zeta_a)$, $a_1 = (2\zeta_1\delta + 1 + k)$, $a_0 = \delta$, $b_3 = 1$, $b_2 = (\delta + 2\zeta_1)$, $b_1 = (2\zeta_1\delta + 1 + k)$ and $b_0 = \delta$ where $\delta = (\sqrt{k}/\zeta_a)$

Figure 6 and **Figure 7** respectively show the curves of Mt1 vs λ (where λ is the ratio of excitation frequency w to the undamped natural frequency w_1 of the system (m_1, k_1) for Case 1 and Case 2 .

2.5. Effect of Variation of Air Damper Spring Rate Ratio *k*

The peak values of Mt1 (at resonance) for increasing values of the air spring rate ratio k and the air damping ratio ζ_a are given in **Table 2** (also refer **Figure 6** and **Figure 7**). It is seen that as the value of air damper spring rate ratio k and air damping ratio ζ_a increase, there is an appreciable reduction in the value of Mt1 at the resonant frequency for the case where the air damper is modeled as a Maxwell type.

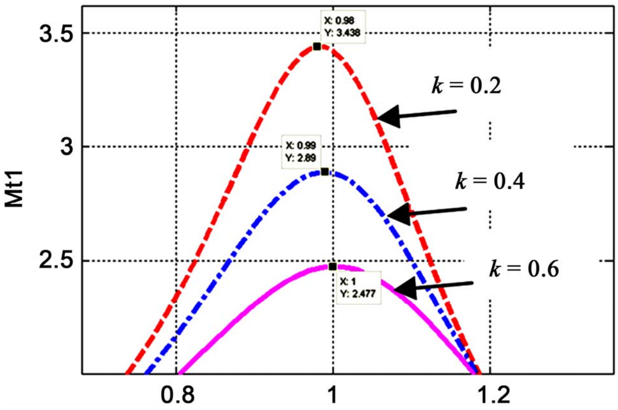

Figure 6. Mt1 vs λ for *k* =0.2, 0.4 and 0.6.

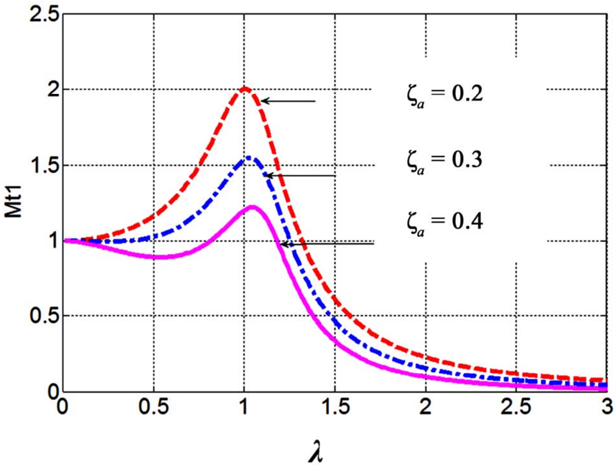

Figure 7. Mt1 vs λ for *ζa* = 0.2, 0.3 and 0.4.

Table 2. Values of spring rate ratio *k* and damping ratio ζ_a varied with air damper modeled as a Maxwell Model.

Peak Values of Mt1	$\zeta_l = 0.133$, $\zeta_a = 0.3$			$\zeta_l = 0.133$, $k = 0.3$		
	k			ζ_a		
	0.2	0.4	0.6	0.2	0.3	0.4
Mt1	3.48	2.89	2.48	2.0	1.55	2.92
λ	0.92	0.96	0.98	0.98	1.08	1.15
Figure No.		6			7	

3. Optimal Value ζ_{aopt} of Air Damping Ratio ζ_a

The air damping is highly effective when the air damper is modeled as Maxwell type (Case 2 of Section 2). As such, Case 2 is taken for optimization of air damping ratio ζ_a The value of Mt1 given by Equation (15) is affected by system damping ratio ζ_1 and the air damper characteristics i) air spring rate ratio k and ii) air damping ratio ζ_a.

Rearranging the equation as a function of ζ_a, we obtain

$$\text{Mt1} = \frac{X_1}{U} = \frac{A2\,\zeta_a^{\,2} + A1\zeta_a + A0}{B2\,\zeta_a^{\,2} + B1\zeta_a + B0} \quad (16)$$

where $A2$, $A1$, $A0$, $B2$, $B1$,$B0$ are the constants containing frequency ratio λ, air spring rate ratio k and system damping ratio ζ_I. Differentiating the rearranged Equation (16) for Mt1 w.r.t. ζ_a and setting it equal to zero *i.e.* $\partial(\text{Mt1})/\partial(\zeta_a) = 0$, we obtain a polynomial in terms of descending powers of ζ_a as

$$C3\zeta_a^3 + C2\,\zeta_a^2 + C1\,\zeta_a + C0 = 0 \quad (17)$$

where C_is are the constant coefficients containing ζ_I, k and λ ($_i$ = 0, 1, 2 and 3). The expressions derived for C_is are lengthy and have not been included in the body of the write-up. The optimal value ζ_{aopt} of ζ_a is obtained by solving the Equation (17) and with the optimal value thus obtained, the values of Mt1 have been determined.

Effect of Air Damping Ratio ζ_a on Amplitude Ratio Mt1 for Various Values of Air Spring Rate Ratio *k*

The values of ζ_{aopt} for the air damper with a Maxwell type model have been obtained for $\zeta_I = 0.133$ and $\lambda = 1$ for different values of *k*. The minimum values of Mt1 (at resonance) for increasing values of the air spring rate ratio *k* respectively are given in **Table 3** (Also refer **Figures 8** to **11**).

4. Experimental Setup

Figure 13 shows the experimental setup designed and developed for dynamic response analysis of the SDOF quarter car suspension system model (refer also **plate 2**). The set up consists of a cam operated mechanism to provide sinusoidal base excitation of the desired amplitude and excitation frequency. The time dependant motion of both the base excitation $u(t)$ and the sprung mass response $x_1(t)$ are sensed and processed by the sensors consisting of LVDTs interfaced with a computer system. The software has been developed to process the input base excitation motion $u(t)$ vs time and the sprung mass response motion $x_1(t)$ vs time. The system also incorporates the facility to control the operating air pressure in the damper system through a computer interfaced system as shown in **Figure 14**. (Also refer **Plate 2**). **Plate 2** shows all the details regarding the laboratory experimental model of a SDOF air damped SDOF quarter-car suspension system. The values of the sprung mass and suspension spring rate are taken respectively as 4.0 kg and 970 N/m.

Air Pressure Control

A computer interfacing system containing the closed loop air pressure control system associated with a set of two LVDTs to sense the suspension mass displacement $x_1(t)$

Table 3. Values of the air spring rate ratio k varied with ζ_1 = 0.133 and λ = 1.

	k					
	0.025	0.050	0.075	0.100	0.200	0.300
$Mt1_{(min)}$	3.763	3.642	3.529	3.422	3.054	2.765
ζ_{aopt}	0.06	0.09	0.11	0.13	0.21	0.27
Figure No.		8			9	
	k					
	0.400	0.500	0.600	0.700	0.800	0.900
$Mt1_{(min)}$	2.538	2.356	2.209	2.089	1.989	1.905
ζ_{aopt}	0.33	0.38	0.44	0.48	0.52	0.57
Figure No.		10			11	

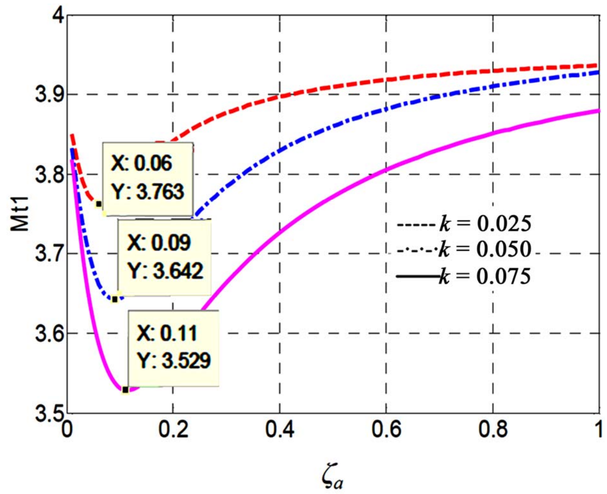

Figure 8. Mt1 vs ζ_a for k = 0.025, 0.05 and 0.075.

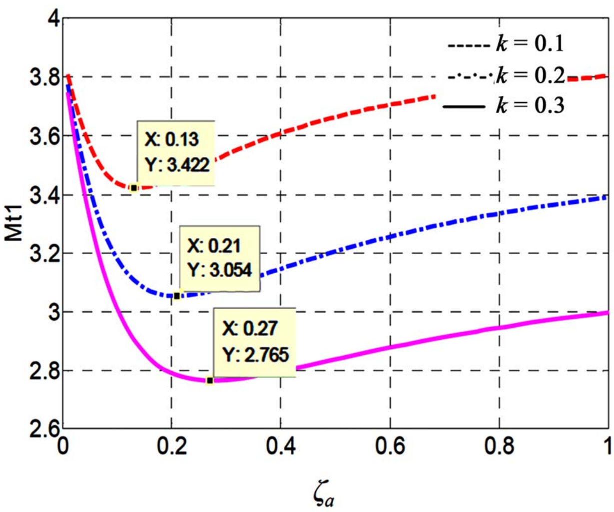

Figure 9. Mt1 vs ζ_a for k =0.1, 0.2 and 0.3.

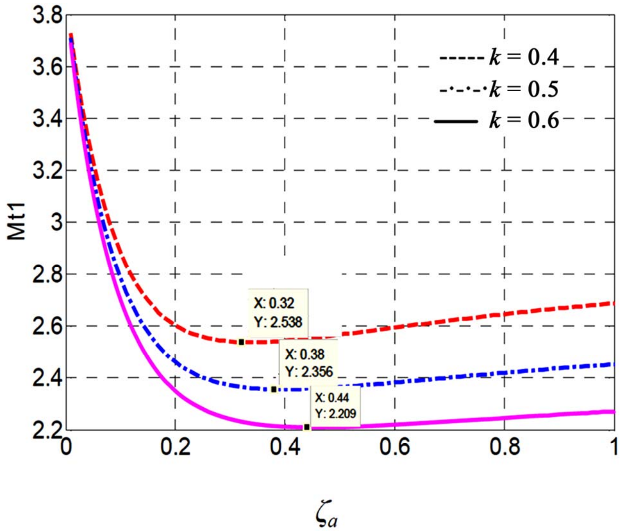

Figure 10. Mt1 vs ζ_a for k = 0.4, 0.5 and 0.6.

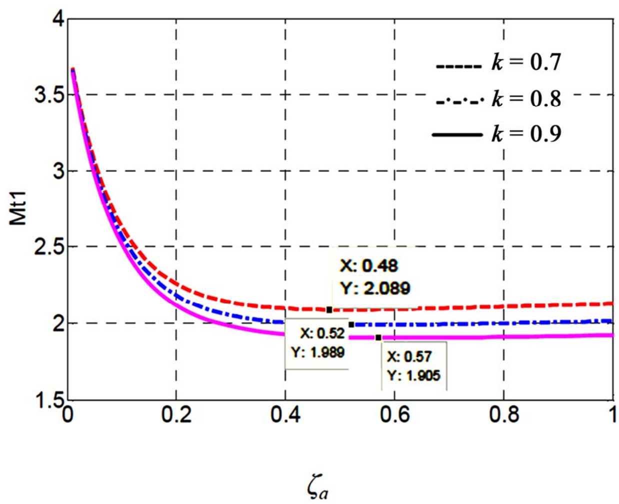

Figure 11. Mt1 vs ζ_a for k = 0.7, 0.8 and 0.9.

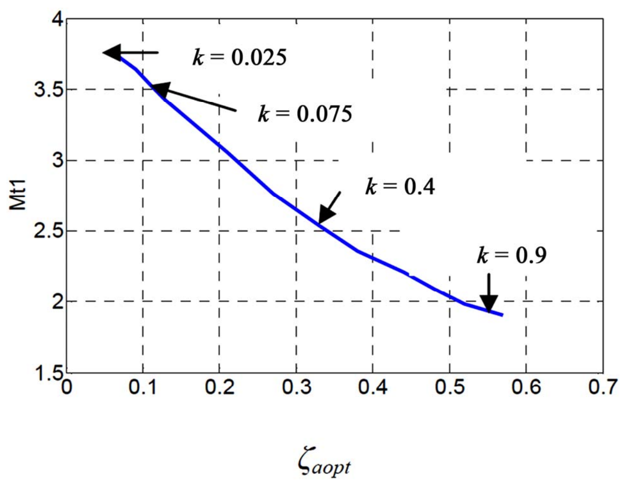

Figure 12. Mt1 vs ζ_a. for k = 0.025 to 0.9.

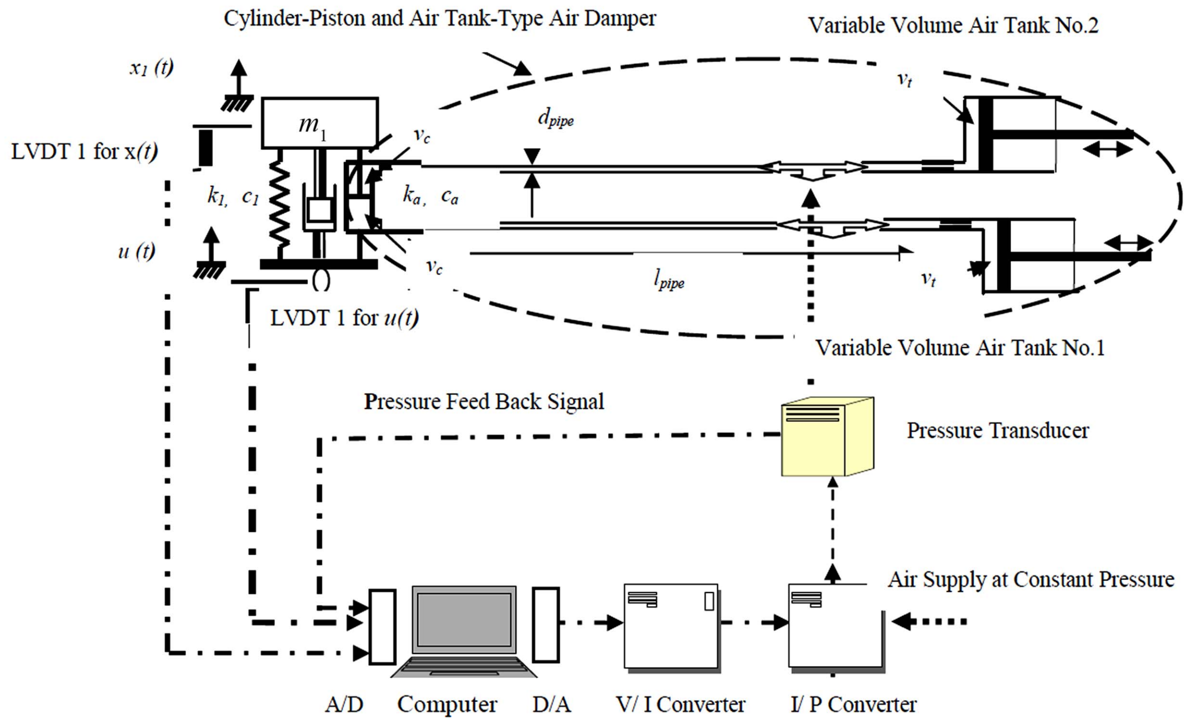

Figure 13. Experimental setup for an air damped SFOF suspension system model.

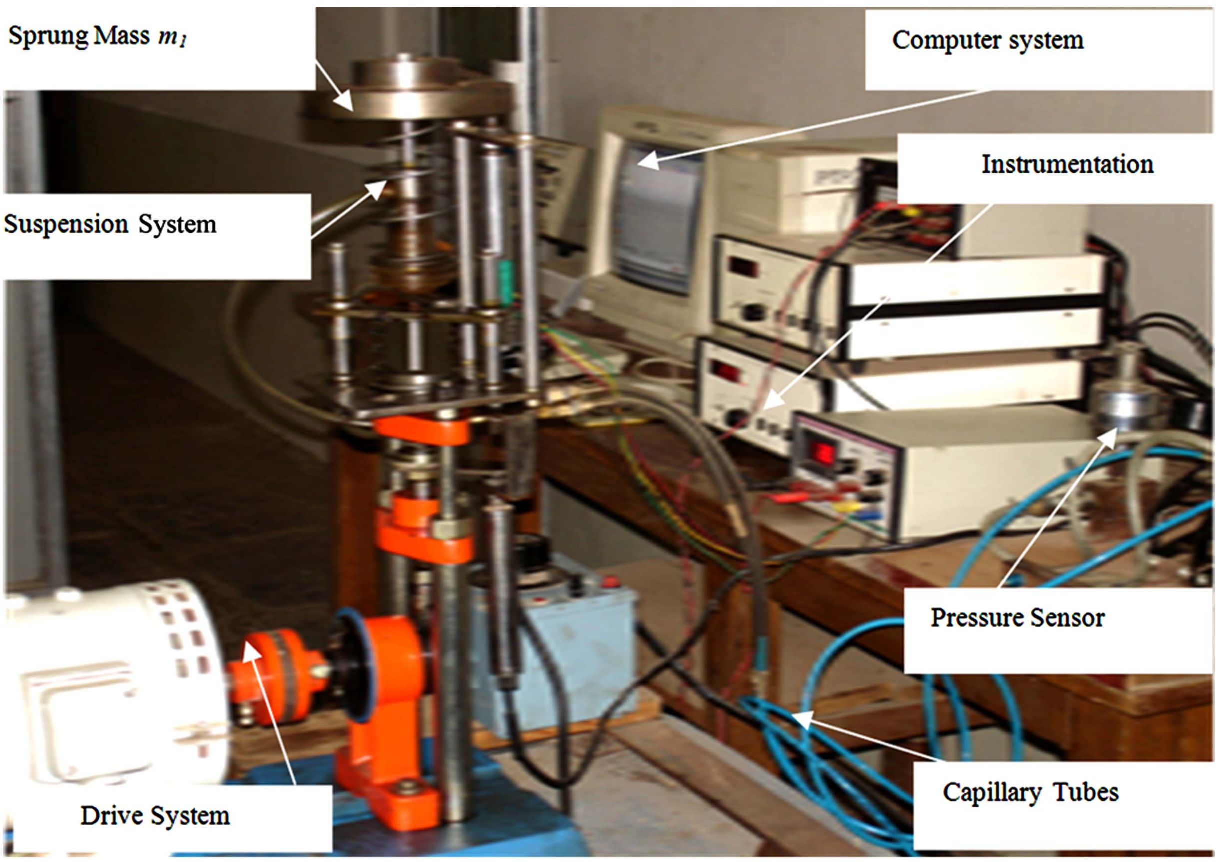

Plate 2. Experimental setup for a SFOF suspension system model with air damper.

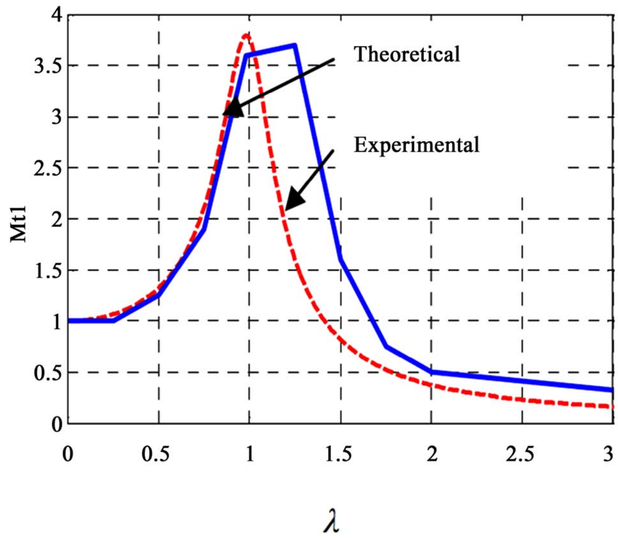

Figure 14. Mt1 vs *λ* case (i) for *ζ*1 = 0 .133.

and base excitation u(t) has been developed .The ratio (*pi/Nt*) plays an important role in controlling the air damping ratio ζ_a in the system. The appropriate value of the ratio (*pi/Nt*), depending on the value of ζ_a desired in the system, can be set by controlling the value of operating air pressure *pi* for a given value of ratio Nt = (v_t/v_c) or keeping the air pressure in the system at the atmospheric pressure and adjusting the value of the term *Nt* by adjusting the tank volume v_t.

5. Experimental Analysis

5.1. Experimental Curves for Motion Transmissibility Mt1 vs Frequency Ratio *λ*

Using the experimental setup shown in **Figure13** and **Plate 2** and by setting the appropriate values of the air spring rate ratio k and the air damping ratio ζ_a, the experimental plots of Mt1 vs λ have been obtained for the SDOF system as i) With system damping only and without air damper (Refer **Figure 14** and **Table 4**) ii) With system damping and air damper, with k = 0.2 (Refer **Figure 15** and **Table 5**).

5.2. Experimental Motion Transmissibility Curves Mt1 vs *λ*, Using Optimal Values of Air Damping Ratio ζ_{aopt}

Table 6 shows the theoretical and experimental minimum values of motion transmissibility Mt1 at resonant frequency (with the air damper set for the optimal air damping ratio ζ_{aopt} at the value of ζ_{aopt} = 0.33 with air spring rate ratio k = 0.4.

Table 4. Theoretical and Experimental Peak Values of $Mt1_{(max)}$ for the Case (i) for ζ_1 = 0.133.

Peak value of	Theoretical	Experimental
$Mt1_{(max)}$	3.798	3.70
λ	0.98	1.25
	Figure 14	

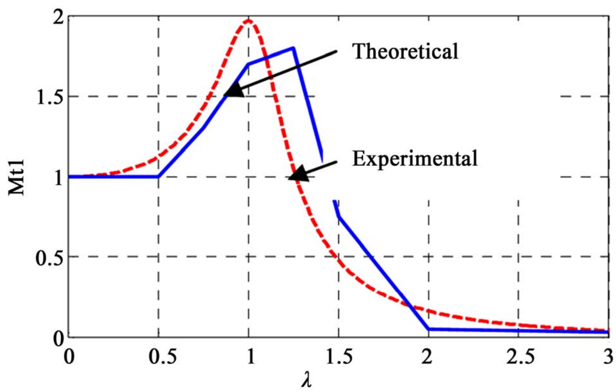

Figure 15. Mt1 vs *λ* for *ζ*1 = 0.133, *k* = 0.2 and *ζa* = 0.2.

Table 5. Theoretical and experimental peak values of $Mt1_{(max)}$ for the case (ii) for ζ_1 = 0.133, k = 0.2 and ζ_a = 0.2.

Peak value of $Mt1_{(max)}$	Theoretical	Experimental
$Mt1_{(max)}$	1.89	1.80
λ	0.98	1.29
	Figure 15	

Table 6. Theoretical and experimental peak values of $Mt1_{(mim)}$ for ζ_1 = 0.133, λ = 1, k = 0.4 and ζ_{aopt} =0.33.

$Mt1_{(min)}$	Theoretical	Experimental
Mt1	2.55	2.10
λ	1.0	1.0
	Figure 16	

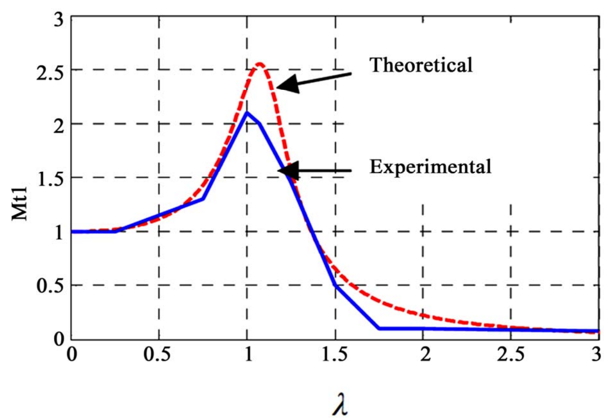

Figure 16. Mt1 vs *λ* for ζ_1 = 0.133, *λ* = 1, *k* = 0.4 and ζ_a opt = 0.33.

6. Conclusions

In this paper, a cylinder-piston and air-tank type air damper has been developed to provide variable air damping for a SDOF quarter car vehicle suspension system. The air damper has been based on the Maxwell type model. The effect of the air damper characteristics *i.e*. air damping ratio ζ_a and air spring rate ratio k on the resonant response of an air damped SDOF vehicle suspension system has been analyzed. It is seen that as the value of the air spring rate ratio k increases, the optimal value ζ_{aopt} increases with decrease in the value of motion transmissibility Mt1. An experimental setup has been developed with an attendant air pressure control system. The values of k and ζ_a for the air damper can be adjusted with the appropriate changes in dimensions of pipe length l_{pipe}, pipe diameter d_{pipe} of capillary pipe between the air damper and the air tank and change in the ratio (*pi/Nt*). From the results of the experimental analysis shown in **Figure 14** and **Figure 15**, it is seen that the experimental values of Mt1 are close to the corresponding theoretical values of Mt1. From **Figure 16**, it is seen that the theoretical and experimental minimum values of Mt1 for ζ_{aopt} = 0.33 with k = 0.4 are in good agreement. The addition of the air damping improves substantially the motion transmissibility characteristics of the sprung mass of the SDOF quarter-car suspension model in the region of resonance.

7. References

[1] R.A. Williams, "Electronically Controlled Automotive Suspension Systems," *Computing and Control Engineering Journal*, Vol. 5, No. 3, 1994, pp. 143-148. doi:10.1049/cce:19940310

[2] Toshihiko Asami and Nishihara, "Analytical and Experimental Evaluation of an Air Damped Dynamic Vibration Absorber: Design Optimizations of the Three-Element Type Model", *Transaction of the ASME*, Vol. 121, 1999, pp. 334-342.

[3] R. D. Cavanaugh, "Air Suspension Systems and Servo-Controlled Isolation Systems," *Hand Book of Shock and Vibration*, 2nd Edition, McGraw-Hill, New York, 1961, pp. 1-26

[4] R. G. Todkar and S. G. Joshi, "Some Studies on Transmissibility Characteristics of a 2DOF Pneumatic Semi-Active Suspension System," *Proceedings of International Conference on Recent Trends in Mechanical Engineering*, Ujjain, 4-6 October 2007, pp. 19-28.

[5] P. Srinivasan, "Mechanical Vibration Analysis," Tata McHill Publishing Co., New Delhi, 1990.

Nomenclature

k_1	stiffness of spring supporting sprung mass
m_1	sprung mass
w_1	$(k_1/m_1)^{1/2}$
ζ_1	system damping ratio
w	applied frequency
λ	frequency ratio = (w/w_1)
d_p	piston diameter
d_c	cylinder bore
l_p	length of the piston
h_p	height of bottom of piston from bottom of the cylinder
d_{pipe}	inside diameter of the capillary pipe
l_{pipe}	length of the capillary pipe
μ_o	viscosity of air
n	index of expansion of the air
k_a	stiffness of air spring
k	spring rate ratio = (k_a/k_1)
w_a	$(k_a/m_1)^{1/2}$
c_a	coefficient of viscous damping provided by the air damper
ζ_a	air damping ratio of air spring
ζ_{aopt}	optimal value of air damping ratio.
$u(t)$	base excitation
$x_1(t)$	dynamic displacement response of sprung mass m_1
Mt1	motion transmissibility of the sprung mass m_1

